

## Feasibility of Improving BWR Performance Using Hydride Fuel

P. Ferroni<sup>2</sup>, M. Fratoni<sup>1</sup>, F. Ginex<sup>1</sup>, F. Ganda<sup>1</sup>, C. Handwerk<sup>2</sup>, E. Greenspan<sup>1</sup> and N. Todreas<sup>2</sup>

<sup>1</sup>University of California, Berkeley, CA 94720

<sup>2</sup>Massachusetts Institute of Technology, Cambridge, MA 02139

**Abstract** - Neutronic and thermal-hydraulic analyses have been performed for U-ZrH<sub>1.6</sub> hydride fueled BWR cores considering a wide range of core design variables: (1) Fuel rod outer diameter – in the range from 0.6 to 1.6 cm; (2) Lattice pitch-to-diameter ratio, P/D – 1.1 to 1.6; (3) Several uranium enrichment levels. The design constraints considered include minimum excess reactivity, negative Doppler coefficient, negative void coefficient, MCPR, peak and average fuel temperatures, peak clad surface temperature, coolant inlet temperature, coolant exit quality, coolant pressure drop, as well as constraints imposed by vibrations and structural considerations.

It was found that U-ZrH<sub>1.6</sub> fuel can significantly simplify the BWR fuel bundle design by eliminating water rods, partial-length fuel rods and wide water channels and by using a single radial enrichment. A 10x10 hydride fuel bundle having the volume of the reference 9x9 oxide fuel bundle can be loaded with 35% more fuel rods having a similar diameter and lattice pitch. As a result of this along with flatter pin-by-pin power distribution the hydride fuel bundle can deliver ~40% higher power density than the reference oxide fuel bundle, provided the core coolant pressure drop could be increased by ~50%. Alternatively, the hydride fuelled core can be designed not to exceed the reference BWR core pressure drop and to deliver the reference power while using ~40% shorter fuel bundles. The hydride fuelled core has a more negative fuel temperature coefficient of reactivity and a less negative void coefficient of reactivity. These trends are expected to enhance the safety and improve the stability of hydride fueled BWRs. A thorough evaluation of hydride fuel and its implementation possibilities in BWRs is recommended.

### I. INTRODUCTION

This paper summarizes work performed within NERI project 02-189.<sup>1</sup> The project objective is to assess the feasibility of improving the economics of light water reactors by using hydride fuel instead of oxide fuel. Most of the effort during the first two years of the project was devoted to the establishment of the overall assessment methodology and to the exploration of optimal PWR core designs.<sup>2-7</sup>

The work reported in this paper focuses on BWR. It summarizes preliminary neutronics and thermal hydraulic analyses. The objective of the neutronic analysis is to identify the acceptable combinations of fuel rod outer diameter, D, and the square lattice pitch to diameter ratio, P/D – to be referred to as “geometry”, of hydride as well as oxide fuels and to quantify the attainable discharge burnup. To be acceptable the geometry has to have negative fuel and coolant temperature coefficients of reactivity as well as negative void reactivity feedback throughout the core life.

The objective of the thermal-hydraulic analysis is to quantify the maximum power density attainable

using different geometries subjected to a number of design constraints. The results from the neutronics and thermal hydraulic analyses will eventually be combined in an economic optimization that will identify the geometry offering the lowest cost of electricity. The hydride fuelled core designs addressed in this work are aimed for new BWR designs; not for retrofitting existing BWRs.

Following a description of the methodology used for this study (Sec. II), we describe the results obtained (Sec. III), derive conclusions and discuss their implications (Sec. IV).

### II. METHODOLOGY

#### II.A Reference BWR

A BWR/5 is used for the reference BWR. A 9x9 fuel bundle is chosen for the reference in lack of non-proprietary data on more advanced bundle and core designs. Table I summarizes key parameters of the reference reactor assumed for this study, based on reference 8.

Table I Key Reference BWR Assumed Parameters

Parameter	Value
<i>Geometry</i>	
Vessel inner radius	3.188 m
Total number of bundles	764
Effective full length fuel rods per bundle	71
Water rod flow area / bundle active flow area	0.0921
Bundle orificing	2 zones: central (648 bundles), periphery (116 bundles)
<i>Operating Conditions</i>	
Core pressure	7.136 MPa
Core inlet temperature	278.3 °C
Core thermal power	3323 MW
Coolant flow rate	13671 kg/s
Radial peaking factor	1.45
Axial peaking factor	1.51
Local peaking factor	1.20 (whole core analysis); 1.23 (subch. analysis)

The fact that the power density of the oxide fuel bundle and core selected for the reference is low relative to more advanced BWR designs does not affect the comparison between hydride and oxide fuels performed in this work, as we are searching for maximum power density oxide and hydride bundle designs using the same methodology.

### II.B Neutronics

There were two parts to the neutronic analysis. The first involved a 1-D scoping study over a wide range of the design variables – the fuel rod outer diameter  $0.6 \leq D \leq 1.6$  and the lattice pitch-to-diameter ratio  $1.1 \leq P/D \leq 1.6$ .<sup>9</sup> Detailed 3-D fuel bundle analysis was then performed for a limited number of promising 10x10 hydride fuel bundles in addition to the reference 9x9 oxide fuel bundle. The analysis was done using MCNP5 Version 1.30 for calculating the power distribution, reactivity coefficients and control systems and using MOCUP<sup>10</sup> for depletion analysis. The oxide fuel bundle geometry and composition were accurately simulated, accounting for water rods, partial length fuel rods, all enrichment levels, Gadolinia as well as bundle box and surrounding water gap.

The hydride fuel considered is TRIGA type U-ZrH<sub>1.6</sub> with 45 wt % U. Information about this fuel and its compatibility with LWRs can be found in reference 6 and references thereof. As the hydrogen density in this fuel is comparable to that in liquid

water in BWR, the hydride fuel bundles considered has no water rods, no partial length fuel rods and no water channel; the bundle pitch is the same as of the reference oxide bundle and is enclosed in a box. These modifications enable to introduce a 10x10 array of rods in the same volume as of the reference 9x9 oxide fuel bundle, giving 96 full length fuel rods per hydride bundle versus ~71 effective full length fuel rods in the reference oxide fuel bundles. The remaining 4 sites house control rods guide tubes; the hydride fuelled cores do not have cruciform control rods.

The axial coolant density distribution was represented using 24 equal length axial zones. Same axial water density distribution – representing a typical core water density distribution of BWR designed by industry, was assumed for all fuel bundles. That is, in this preliminary phase of feasibility study the neutronic and thermal-hydraulic analyses were not fully coupled.

24 depletion zones were considered for the reference oxide bundle, corresponding to 8 groups of fuel rods and three average axial enrichments per group. Being of significantly more uniform design, only 9 depletion zones were considered for hydride fuel bundles – 3 equal length axial and 3 radial zones. The fraction of the bundle power generated in each depletion zone was calculated at each burnup step by MOCUP. A 4 equal size batch fuel management was assumed for estimating the discharge burnup and core average k and reactivity coefficients. Table II gives the fraction of the core power and the average power per fuel bundle assumed for each batch based on information from actual BWR design. The corresponding core average bundle power is 4.31 MW<sub>th</sub>, regardless of the fuel type.

Table II Core Power per Batch

Batch number	Fractional power	Power per bundle [MW]
1 <sup>st</sup>	31.42%	5.40
2 <sup>nd</sup>	27.41%	4.73
3 <sup>rd</sup>	24.61%	4.17
4 <sup>th</sup>	17.11%	2.95

The achievable burnup was taken to be that burnup for which the above power weighting procedure gave k of 1.05 – conservatively assuming 5% radial leakage probability. The 4-batch average core reactivity,  $\rho$ , and k were estimated from

$$\rho = \sum_{i=1}^n \rho_i f_i \quad \text{or} \quad \frac{1}{k} = \sum_{i=1}^n \frac{f_i}{k_i} \quad (1)$$

where  $\rho_i$  is the reactivity pertaining to batch i and  $f_i$  is the fraction of the core power generated by batch I (from Table II). Likewise for the multiplication factor

k. Table III compares the discharge burnup thus obtained relative to the burnup obtained using two simplified procedures for estimating the effective core k: (a) as above but assuming uniform power, i.e.,  $f_i=1/n$  at the RHS of Eq. (1) for k; (b) direct averaging of the multiplication factor  $k = \frac{1}{n} \sum_{i=1}^n k_i$ .

Both of these procedures overestimated the final BU.

Table III Achievable Burnup Dependence on Batch Averaging; Reference Oxide Bundle

Averaging procedure	Burnup [GWD/tHM]	Residence time [days]
Variable Power Reactivity	43.5	1740
Uniform Power Reactivity	44.0	1760
Uniform Power Direct k	46.0	1840

A similar averaging procedure was applied to determine the reactivity worth of the control systems and the reactivity coefficients.

Additional constraint was imposed when accounting for burnable poisons – the Beginning Of Life (BOL) core average multiplication factor is to equal that of the reference oxide core that uses gadolinium.

The statistical uncertainty in calculating k was  $< 5 \cdot 10^{-4}$  such that, after propagation through the k averaging procedure, the uncertainty in the core average k was  $< 2 \cdot 10^{-3}$ .

### II.C Thermal-Hydraulic Analysis

The thermal hydraulic analysis was also performed in two parts – a *whole core analysis* was first performed covering a wide range of D and P/D ratios – nearly 400 geometries, altogether. *Subchannel analysis* was then performed in greater detail for a limited number of fuel bundles. The VIPRE-EPRI code<sup>11</sup> was used for this analysis.

For the oxide fuel whole core analysis, the fuel bundles are assumed to contain a single water rod, such that the ratio between its cross section area and the bundle active flow area (water rod excluded) equals that of the reference bundle design. The fuel box dimensions are fixed; it is separated from the neighboring boxes by a constant width bypass channel.

A greater design freedom was assumed for the first round of hydride fuelled core analysis – the fuel bundle transverse dimensions were allowed to vary. As described above, the hydride core does not contain water rods and bypass flow channels but is

provided with control rod guide tubes within the bundle as in PWR and is encased in a box, as in BWRs.

Both the oxide and hydride cores are assumed contained in a BWR/5 vessel dimensions. In spite of the different fuel and bundle designs, the power peaking factor is assumed the same for the whole core analysis.

The constraints imposed for the whole core analysis are summarized in Table IV:

*MCPR.* The minimum critical power ratio of 1.140 is that value derived for the reference oxide core using the VIPRE thermal-hydraulic analysis with the Hench-Gillis correlation. This correlation, also known in VIPRE as the EPRI-2 correlation, is a critical quality-boiling length correlation developed in 1981 for EPRI by S. Levy Inc. Its stated range of validity encompasses the entire design range considered in this study. Even though an MCPR of 1.140 is smaller than the commonly accepted value for BWRs –  $1.24 \div 1.28$ ,<sup>8</sup> its use provides for a consistent comparison between the new bundle designs and the reference design.

Table IV Constraints Imposed for the Whole Core Analysis

	Oxide core	Hydride core
<i>Thermal Hydraulic Constraints</i>		
MCPR	1.140	1.140
Fuel centerline T <sup>(a)</sup> (°C)	2805	750
Fuel average T <sup>(a)</sup> (°C)	1400	N.A.
Clad surface T <sup>(a)</sup> (°C)	349	349
Core pres. drop (MPa)	0.2620	0.2620
Vibration ratio	0.021	0.021
Core power/Flow rate (kJ/kg)		243.07
<i>Structural Constraints</i>		
Number of bundles	N.A.	1222
Bundle weight (kg)	N.A.	361

<sup>(a)</sup> at steady state N.A.: Not Applied

*Fuel centerline / average temperature.* UO<sub>2</sub>: 2805°C and 1400°C to prevent fuel melting and exceeding 5% fission gas release, respectively.<sup>12</sup> UZrH<sub>1.6</sub>: 750°C prevents excessive hydrogen dissociation.<sup>13</sup>

*Clad surface temperature.* 349°C was chosen to assure sufficient margin between the oxide corrosion layer thickness that unavoidably forms during steady state operation and the maximum oxide thickness allowed during LOCA severe accidents. According to the NRC Regulation 10 CFR 50.46, the maximum

thickness shall nowhere exceed 17% of the total cladding thickness before oxidation.

**Core pressure drop.** The maximum allowed core pressure drop is assumed to be 50% higher than that of the NMP2 reference core. Industry experts we consulted suggested this as the pressure drop to be attainable within few years as a result of improvements in pump technology and use of additional pumps. This trend is already observed in ABWR II – its designed pumps head is 0.347 MPa versus 0.287 MPa in ABWR. In fact, the additional 0.06 MPa of ABWR II already provides ~25% of the core pressure drop increase assumed.

**Vibration ratio.** Defined as  $y_{max}/D$  where  $y_{max}$  is the peak transversal rod vibration amplitude while  $D$  is the rod outer diameter. A modified version of the Paidoussis correlation<sup>14</sup> was used to compute this parameter. The vibration amplitude is conservatively estimated by neglecting the presence of the fuel inside the rods. The maximum allowed value was chosen based on typical limits encountered in the reactor design literature.

**Power/Flow.** To limit the average exit quality, and thereby make two-phase instability phenomena less likely, the ratio between the core power and the coolant flow rate is maintained constant and equal to that of the reference core, i.e. 243.07 kW/(kg/s).

**Number of bundles.** To prevent excessive fuel handling and a consequent long refueling time the number of bundles has an upper limit of 1222, corresponding to 1.6 times the number of bundles in the reference core.

**Bundle Weight.** Due to limited crane load capacity, the maximum allowed bundle weight was chosen to be 1.4 times the reference bundle weight, i.e. 1.4×258 kg. Canister and fuel spacer weight are not accounted for both the reference and new designs.

The computational analysis of multiple combinations of geometries and operating parameters was performed by interfacing the thermal hydraulic analysis code VIPRE-EPRI with MATLAB that generates the VIPRE input files, executes VIPRE and manages the output data. This interface, called VAMPIRE (VIPRE And MATLAB Programming InteRfacE), was developed for PWRs by Blair<sup>15</sup> and Malen<sup>16</sup> and adjusted for BWRs by Handwerk.<sup>17</sup>

**Subchannel analysis** was performed for six fuel bundles – the reference oxide 9×9 bundle and five 10×10 hydride bundles – all having the same overall bundle dimensions but may differ in D, P/D and pin-wise power distribution – the peak to average pin power ratio is 1.23 for the reference oxide bundle versus 1.25 (“Worst Case”) and 1.05 (“Best Case”) for the hydride fuel bundles. The Worst Case corresponds to use of Gadolinia whereas the Best

Case corresponds to use of IFBA for the burnable poison. The use of such burnable poisons also results in the reduction of the required number of control rods to 4 per bundle. The fuel-clad gap was assumed, for all bundles, filled with a liquid metal<sup>5</sup> having a thermal conductivity of 35 W/m K.

The thermal hydraulic constraints assumed for the subchannel analysis are summarized in Table V; they are similar to those of Table IV with the following exceptions: (1) No constraints are applied on the number of bundles and bundle weight. (2) The pressure drop limit is slightly lower – 0.2275 vs 0.2620 MPa. This is because the subchannel analysis models the bundle active length only, not accounting for the friction pressure drop in the unheated length of the coolant channel. (3) The MCPR is lower – 1.106 vs 1.140. Although the procedure used for determining the MCPR is the same as that used for the whole core analysis, the peak pin power used for the reference bundle is slightly higher than that assumed for the whole core analysis. (4) The vibration limit is not applied, since the bundle designs examined in the subchannel analysis are far from the vibration-limited D-P/D geometries. (5) In place of the Power/Flow ratio, the subchannel averaged exit quality is used as a constraint. The corresponding limit, 23.73%, is the subchannel averaged exit quality for the reference oxide bundle. However, in some cases, the exit quality is allowed to exceed this limit. This is due to the investigative character of the subchannel analysis and to the fact that a small increase of the exit quality might be accepted without resulting in two-phase instability phenomena. For each case an estimate of the Decay Ratio (DR), which is a measure of how quickly two-phase instability phenomena tend to die-out, is also performed. The DR is estimated as 130% of the DR calculated assuming a uniform axial power distribution. The limit chosen, 0.5, is well below the maximum allowed value for a single channel – 0.8.<sup>18</sup>

Table V Constraints used in the Subchannel Analysis

	Ref. oxide bundle	Hydride bundles
<i>Thermal Hydraulic Constraints</i>		
MCPR	1.106	1.106
Fuel centerline T <sup>(a)</sup> (°C)	2805	750
Fuel average T <sup>(a)</sup> (°C)	1400	N.A.
Clad surface T <sup>(a)</sup> (°C)	349	349
Active bundle ΔP (MPa)	0.2275	0.2275
Decay ratio	0.5	0.5
Subchannel avg exit quality	0.2373	0.2373

<sup>(a)</sup> at steady state

N.A.: Not Applied

### III. RESULTS

#### III.A Neutronic Analysis

A detailed 3-D neutronic analysis was performed for the oxide and hydride fuel bundles to determine attainable discharge burnup, pin-by-pin power distribution, axial power distribution, reactivity coefficients, reactivity worth of control elements and burnable absorber effects. Table VI compares the hydride fuel bundle offering the largest discharged BU against the reference oxide fuel bundle without accounting for burnable poisons (BP).

The maximum BU 10x10 hydride fuel bundle pitch is similar but the fuel rod diameter is somewhat larger than those of the reference oxide fuel bundle. Its pin-by-pin power distribution is very flat – the pin-wise power peaking factor does not exceed 1.05 during the entire cycle against a minimum of 1.10 for the oxide fuel. A drawback for this 10x10 bundle is a large BOL axial power peaking factor – 2.13 compared to 1.64 for the oxide. An axial fuel enrichment distribution could easily suppress that peak. For example, it was found that using 5.17% in the top one third and 4.67% in the bottom two third of all the fuel rods will reduce the axial peaking factor to 1.723. A further optimization may be required but the main indication is that the high axial peaking can be reduced while keeping the bundle design significantly simpler as compared with the oxide bundle design.

Table VI Oxide and Hydride Fuel Neutronic Performance Comparison. Not Accounting for BP

System	Oxide 9x9	Hydride 10x10
Number fuel rods	70.67	96
Fuel rod OD [cm]	PI <sup>(a)</sup>	1.2413
P/D	“	1.1500
Control system	Control blades	4 control rods
Average enrichment	3.9%	5%
Relative HM per bundle	1.0	0.68
Burnup [GWD/MTHM]	43.5	52.0
Residence time [days]	1740	1412
BOL axial power peaking factor	1.6414	2.1319
BOL Pin power peaking factor	1.1017	1.0440

<sup>(a)</sup> Proprietary information

Core (i.e., 4 batch) average beginning of cycle reactivity coefficients calculated for the reference oxide and for the maximum BU hydride fuel bundles, without burnable poisons, are summarized in Table

VII. An average void fraction of 40% is assumed for the nominal conditions. All temperature and void coefficients considered are negative. The hydride fuel offers more negative prompt reactivity feedback due to fuel heat up and not as negative small void reactivity coefficient – both trends are expected to improve reactor safety and stability.

Table VII Oxide and Hydride Fuel Reactivity Coefficients at BOC. 4 Batch Average; no BP

System	Oxide 9x9	Hydride 10x10
Fuel temperature	-4.6 pcm/K	-6.7 pcm/K
Small void (45%)	-0.43 Δk%	-0.25 Δk%
Large void (90%)	-4.65 Δk%	-4.75 Δk%

Although the neutronic analysis revealed that P/D of 1.15 offers the maximum hydride fuel discharge burnup, the thermal-hydraulic analysis suggested that higher power could be generated with an increase in P/D. Then fixing the pitch and decreasing the fuel rod outer diameter to nearly the reference oxide fuel diameter, P/D was increased to 1.30 while the negative reactivity coefficients were maintained. As a result the burnup dropped to 48 GWD/MTHM and the residence time to 1012 days. However, by increasing the fuel enrichment to 7.70% it is possible to obtain a cycle as long as that of the reference oxide fuel with the 10x10 high power density hydride fuel bundle. The corresponding discharge burnup is 82.5 GWD/MTHM.

Four control rods interspersed between fuel rods in the 10x10 hydride fuel bundle were found to provide a shut-down reactivity margin that is comparable to that of the control blades in the reference oxide fuel design. B<sub>4</sub>C with natural boron was used as the neutron absorber. The preferred location of the 4 control rods are positions C-3, C-8, H-3 and H-8.

Table VIII compares the penalty imposed by use of burnable poisons on the attainable discharge burnup and on the power peaking factors of a number of hydride fuel bundle designs relative to the reference oxide fuel bundle. In the reference oxide bundle Gadolinia of ~5 wt% is mixed with the fuel in 12 out of 71 effective full length rods per bundle. The gadolinium is of natural composition. The use of burnable poison in hydride fuel was studied for the neutronic optimal geometry of P/D=1.15. The amount of poison loaded into each fuel bundle was that which makes the average core multiplication factor at BOL 1.07 – as in the reference oxide fuel core. This constraint was coupled with the EOL constraint of a 4-batch average multiplication factor of 1.05. The required amount of gadolinium in hydride fuel, assumed loaded in the metallic form,

was found about 2.87 wt% when added to 8 out of the 96 fuel rods. These rods were dispersed in the core similarly to the scheme of loading Gadolinia in the reference oxide fuel bundle. The localization of the gadolinium introduces large peaks in the BOL pin-by-pin power distribution, similar to the peaks encountered in oxide fuel bundle designs.

Table VIII Burnable Poisons Effects

System	Oxide + Gd	Hydr.+ Gd	Hydr.+ IFBA	Hydr. + <sup>167</sup> Er
BU loss [GWD/MTHM]	6	6	6	9
Burnup [GWD/MTHM]	37.5	46	46	43
Residence time [days]	1482	1242	1162	1248
Axial power peaking, BOL	1.845	2.609	2.295	3.003
Pin power peaking, BOL	1.228	1.246	1.052	1.050

Much flatter pin-wise power distributions were calculated when using IFBA or erbium as burnable poisons; both were uniformly distributed over all the hydride fuel rods of the bundle. For simplicity the IFBA was modeled uniformly dispersed in the fuel rather than as a thin layer on the fuel surface. A single pin depletion benchmark verified that this simplification is acceptable. IFBA is in the chemical form of ZrB<sub>2</sub>, uses natural boron and has an initial loading of 0.22 wt% of the fuel.

Erbium of natural composition was added to the fuel in the form of ErH<sub>3</sub> in the amount of 0.55 wt%. Although the pin-by-pin power distribution remains very uniform, the achievable burnup is drastically reduced by 12 GWD/MTHM. The reason of this strong burnup penalty is the fact that, of the natural isotopes of erbium, only <sup>167</sup>Er is a strong neutron absorber; its abundance is ~23%. During operation it is kept being generated by (n,γ) reactions on <sup>166</sup>Er that makes 33.6% of the natural erbium. Had it been practical to fully enrich erbium in the isotope 167, the achievable burnup was found limited to 43 GWD/MTHM; less than with gadolinium and IFBA.

The axial power peaking factors for hydride fuel, shown in Table VIII, are significantly larger than that of the reference oxide fuel. However, as discussed above, it is likely to be relatively simple to control this axial peaking by axial partition of the fuel enrichment or burnable poison concentration without much penalty to the hydride bundle designs. All the hydride fuel designs with burnable poisons offer negative reactivity coefficients over the entire cycle length and are, therefore, neutronically feasible.

### III.B Thermal Hydraulic Analysis

#### Whole Core Analysis

Figure 1 shows the maximum attainable power of oxide cores as a function of D and P/D. The maximum power is 3854 MW<sub>t</sub> – ~16% higher than of the reference design; it is achieved by three geometries having the same rod diameter but different pitch in 12×12 fuel bundles. This trend is consistent with the industry practice to shift to a larger number of fuel rods of a smaller diameter per bundle.

The attainment of the higher power level is due to the larger number of fuel rods per core as is verifiable from Figure 2. It compares the power, the Linear Heat Generation Rate (LHGR) and the number of fuel rods of the core configurations examined with those of the reference core. The lines that appear in plots (a), (b) and (c) are the loci of ratios of 1.0. Plot (d) in Figure 2, a superposition of the previous three, shows that the high power region is located where the number of fuel rods is the maximum. The contribution given by increasing the number of rods is more significant than that from the combination of a larger number of rods AND a higher LHGR that characterizes the narrow region between the two unity lines of subplots (b) and (c); the LHGR of the D-P/D pairs offering the maximum power is lower than the reference.

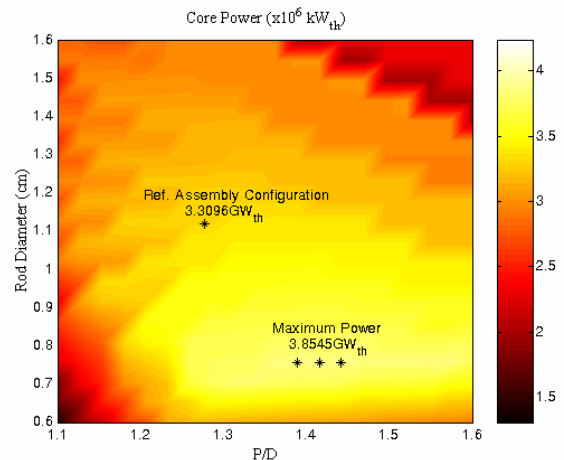


Figure 1: Maximum achievable power; oxide

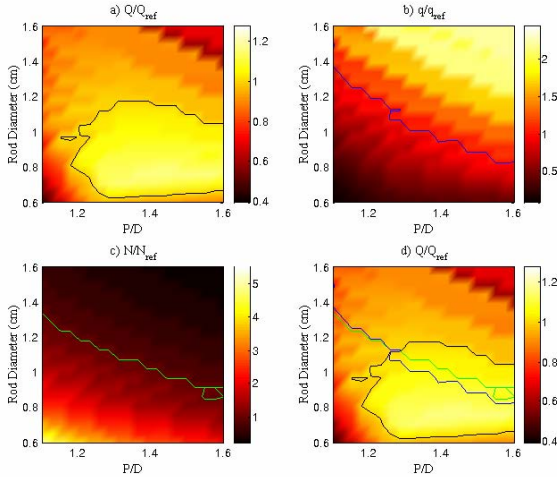


Figure 2: (a) Power, (b) LHGR, (c) Number of rods relative to the reference oxide core value, (d) Superposition of (a), (b) and (c)

The power limit imposed by the constraints is shown in Figure 3. The constrained D-P/D sub-space appears as white. Figure 3 shows that the achievable power level is constrained primarily by the MCPR. The fuel centerline temperature and the clad surface temperature are never constraining and, therefore, are not displayed in Figure 3.

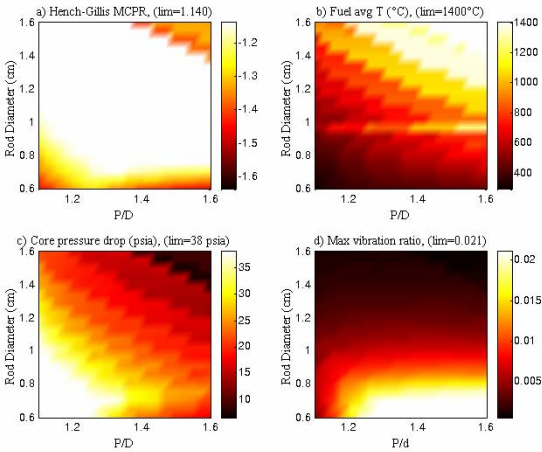


Figure 3: Limiting constraints; oxide core

The maximum power attainable from the hydride fuelled cores is shown in Figure 4. The power of the reference D-P/D geometry, 4057MW<sub>t</sub>, is ~22% higher than that of the reference oxide core, 3310 MW<sub>t</sub>. The maximum power achievable with a hydride core, 4839 MW<sub>t</sub>, is ~25% higher than the maximum power achievable with an oxide core – 3854 MW<sub>t</sub>.

Figure 5 and Figure 6 are analogous to Figure 2 and Figure 3. Again, as Figure 4 and Figure 5 (d)

illustrate, the D-P/D pair having the maximum power is not located in the region included between the unity line of Figure 5 (b) and that of Figure 5 (c).

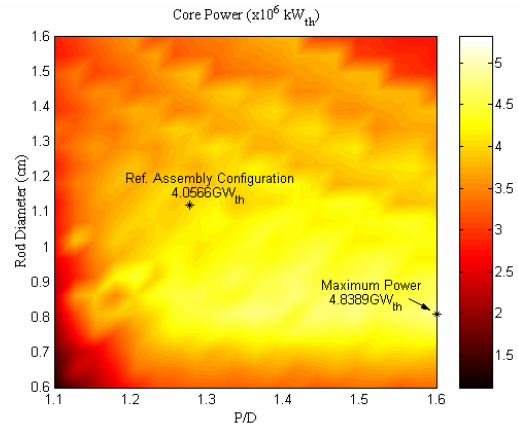


Figure 4: Maximum achievable power; hydride cores

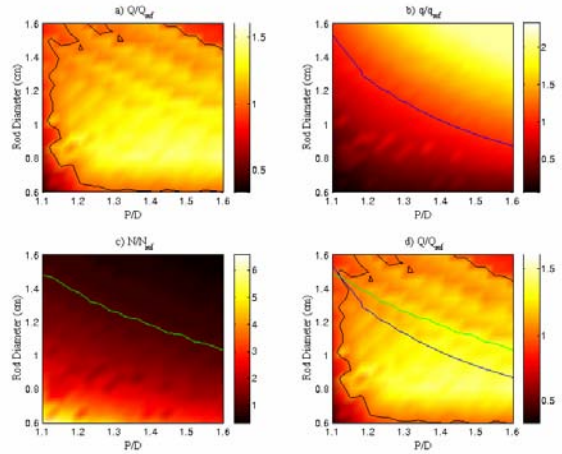


Figure 5: (a) Power, (b) LHGR and (c) Number of rods of hydride cores relative to the reference oxide core, (d) Superposition of (a), (b) and (c)

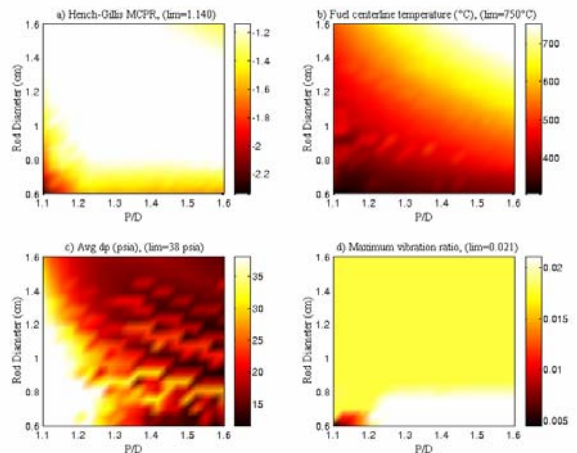


Figure 6: Limiting constraints; hydride cores



The whole core analysis comparison between hydride and oxide core performance reported above, although indicative of the right trends, is not accurate enough. This is because the oxide fuel bundles were restricted to a single dimension whereas the hydride fuel bundle dimensions was a variable and the effective core cross section area was, consequently, not identical. The subchannel analysis reported below is free of this inconsistency. However, it does not explore the full D-P/D design space.

#### Subchannel Analysis

Subchannel analysis was applied to five 10x10 hydride fuel bundles and to the 9x9 reference oxide fuel bundle. Table IX compares design and performance characteristics of the hydride fuel bundle offering the highest power with those of the reference oxide fuel bundle. It is seen that the hydride fuel power is 46% higher than that of the reference oxide bundle, both bundles taking identical core volume. Had the pressure drop constraint of the oxide core been increased from the reference 0.1544 MPa to 0.2275 MPa assumed for the new designs, its power level would increase to 6.5916 MWth while its exit quality would decrease to 18.16%. The hydride fuel bundle power is 40% higher than that of the elevated pressure drop oxide fuel bundle.

The oxide fuel bundle power is limited by the MCPR constraint while the hydride fuel bundle power is limited by the pressure drop constraint. The relatively low peak temperature of the hydride fuel is due to its high thermal conductivity – nearly 5 times higher than that of oxide fuel. Liquid metal bonding is assumed for both the hydride and oxide fuels.

Based on the whole core analysis reported above it is expected that the power level of both the oxide and hydride fuel bundles will be increased by using larger number of fuel rods of a smaller diameter – as actually being done by industry – the evolution of BWR fuel bundles is characterized by continuously increasing number of fuel rods (oxide) per bundle.

#### IV. CONCLUSIONS

It is found possible to design hydride fuel bundles for the BWR that are significantly less heterogeneous than present day oxide fuel bundles and that can operate at a remarkably higher power density without violating any of the steady-state design constraints used for BWR; relative to the reference oxide fuel bundle, hydride fuel bundles using comparable fuel rod diameter and comparable lattice pitch offer a calculated power density increase of approximately 40%, provided the core coolant pressure drop could be increased from the reference

Table IX Power Attainable from Selected Bundles Predicted by Subchannel Analysis

Characteristic	Ox 9x9 (ref)	Hyd-4 10x10
Fuel rod diameter, D (cm)	PI <sup>(a)</sup>	1.1178
Fuel rod pitch (cm)	“	1.4532
Active flow area ( $\times 10^{-3}$ m <sup>2</sup> )	“	11.3854
P/D	“	1.3000
Clad thickness (cm)	“	0.0673
Fuel Pellet Diameter (cm)	“	0.9356
Control rod guide tube outer/inner diameter (cm)	N.A.	1.3894/ 1.2108
Effective # of fuel rods	71	96
Number of grid spacers	7	7
Grid spacer loss coefficient	1.20	1.20
Lower tie plate loss coef.	9.4609	9.4609
Upper tie plate loss coef.	0.3751	0.3751
Flow area orificing coef.	21.089	21.089
Active bundle $\Delta P$ (MPa)	0.1544	0.2275
Exit quality	23.73	23.73
MCPR	1.106	1.114
Fuel peak temperature (°C)	1366	545
Bundle power (MWth)	6.3067	9.2067

<sup>(a)</sup> Proprietary information

BWR design value of 0.1544 MPa to 0.2275 MPa. Alternatively, the hydride core can be designed to deliver the nominal BWR power and have close to the reference BWR pressure drop (~0.2275/1.4 MPa) using fuel bundles that are ~40% shorter than the reference. Most of the power density increase of hydride fuel is attributable to the increase (of ~35%) in the number of fuel rods per core volume. An additional few percent increase is due to the flatter pin-wise power distribution of hydride fuel bundles.

The hydride fuel bundles have greater discharge burnup but reduced HM inventory per bundle. Consequently, the hydride fuel need have higher uranium enrichment to provide the reference cycle length. A potentially promising approach for obtaining long cycles is to use thorium-containing hydride fuels<sup>6</sup> not examined in the present work; the HM contents of thorium-based hydride fuel is more than double that of the U-ThH<sub>1.6</sub> fuel considered in this work; it is even larger than that of oxide fuel.

The fuel temperature coefficient of reactivity of the hydride fuel bundle designs considered is more negative than that of the reference oxide fuel bundle whereas the void coefficient of reactivity of the hydride fuel bundle is less negative. These trends are expected to enhance the safety and improve the stability of hydride fueled BWRs. Adequate shutdown margin can be provided by incorporating four B<sub>4</sub>C control rods per 10x10 hydride fuel bundle.



The feasibility study need be refined and extended before sound conclusions could be withdrawn on the possible benefits from using hydride fueled BWR cores. Future undertakings should include coupled neutronic - thermal hydraulic analysis, transients and accidents analysis, as well as economic analysis. A number of important feasibility issues need to be assessed including (1) elimination of large water gaps around the fuel bundles and the replacement of cruciform control blades by clusters of control rods. (2) Compatibility of hydride fuel with BWR water and clad.

### ACKNOWLEDGMENT

This work was supported by US DOE NERI under award number DE-FG07-02SF22615. Help provided by Dr. Russ M. Fawcett of GNF is highly appreciated.

### REFERENCES

1. E. Greenspan, N. Todreas and B. Petrovic, "Use of Solid Hydride for Improved Long-Life LWR Core Designs," *NERI Project Number 02-189, 2002*.
2. E. Greenspan, H. Garkisch, J. Malen, M. Moalem, D. Olander, B. Petrovic, Z. Shayer and N. Todreas, "Preliminary Assessment of Possibilities for Improving the Performance of LWRs Using Hydride Fuel," *Transactions American Nuclear Society*, \_\_ **89**, 381-382, November 2003.
3. Z. Shayer and E. Greenspan, "Physics of U-ZrH<sub>1.6</sub> Fuel in PWR," *Proc. of the Reactor Physics Topical Meeting, PHYSOR-2004*, Chicago, IL, April 2004.
4. J. A. Malen, N. E. Todreas, A. Romano, "Thermal Hydraulic Design of Hydride Fueled PWR Cores," *Proc. 6<sup>th</sup> Int. Conf. on Nuclear Thermal Hydraulics, NUTHOS-6*, Nara, Japan, October 4-8, 2004. Paper ID: N6P216.
5. E. Greenspan, F. Ganda, H. Garkisch, J. Malen, B. Petrovic, A. Romano, Z. Shayer, C. Shuffler, N. Todreas and J. Trant, "Optimization of UO<sub>2</sub> Fueled PWR Core Design", *Proc. 2005 International Conference on Advances in Nuclear Power Plants; ICAPP-2005*, Seoul, Korea, May 15-19, 2005.
6. F. Ganda, E. Greenspan, "Incineration of Pu in PWR Using Hydride Fuel," *Proc. 2005 International Conference on Advances in Nuclear Power Plants; ICAPP-2005*, Seoul, Korea, May 15-19, 2005.
7. F. Ganda and E. Greenspan, "Plutonium Incineration Capability of Hydride Versus MOX Fuel in PWR" *Proceedings of GLOBAL'05*, Tsukuba, Japan, October 9-13, 2005.
8. Nine Mile Point Unit 2, Updated Safety Analysis Report (USAR), Rev.16, October 2004.
9. F. Ginex, F. Ganda, M. Fratoni and E. Greenspan, "One-Dimensional Neutronic Analysis of BWR Hydride Fuel Bundles," Submitted to *Advances in Nuclear Analysis and Simulation, PHYSOR 2006*, Vancouver, BC, Canada, September 10 - 14, 2006.
10. R.L. Moore, B.G. Schnitzler, C.A. Wemple, R.S. Babcock, D.E. Wessel, "MOCUP: MCNP-ORIGEN2 Coupled Utility Program," *Idaho National Engineering Laboratory Report INEL-95/0523*, September 1995.
11. C. Stewart. "VIPRE-01: A Thermal Hydraulic Code for Reactor Cores. Vol.2: User's Manual", August 1989.
12. M.S. Kazimi, N.E. Todreas: "Nuclear Systems I, Thermal Hydraulic Fundamentals", *Taylor & Francis*, 1993.
13. H.D. Garkisch, B. Petrovic, "Reference Data and Constraints for Uranium-Zirconium-Hydride and Uranium-Thorium Hydride Fuels for Light Water Reactors", *Westinghouse Electric LLC, Rev.6*, March 9, 2003.
14. M.P. Païdoussis: "Fluid-Structure Interactions, Slender Structures and Axial Flow", Volume 2, *Academic Press, Inc.*, p. 869, 1998 <c2004>.
15. S. Blair, "Thermal Hydraulic Performance Analysis of a Small Integral PWR Core", Engineers Thesis, *MIT, Department of Nuclear Engineering*, September 2003.
16. J. A. Malen, N. E. Todreas, & A. Romano, "Thermal Hydraulic Design of Hydride Fueled PWR Cores," *MIT-NFC-TR-062*, MIT Department of Nuclear Science and Engineering Report and associated computer files, March 2004.
17. C. Handwerk, "Preliminary Thermal Hydraulic Analysis of a Hydride Fueled Boiling Water Reactor", *NERI02-189-MIT-9*, January 2005.
18. GE Nuclear Energy, "ESBWR Design and Technology Reprints of Recent Papers", Volume 3, January 1999.